Adv. Polar Upper Atmos Res., 16, 181-192, 2002

A new method for monitoring and removing SuperDARN radar DC offsets

Akira Sessai Yukimatu, Masaki Tsutsumi,
Hisao Yamagishi and Natsuo Sato

National Institute of Polar Research, Kaga 1-chome, Itabashi-ku, Tokyo 173-8515

Abstract DC offsets in quadrature outputs (I/Q signals) pertinent to the SuperDARN HF radars can cause problems in determining and analysing auto-correlation functions, cross-correlation functions and raw time series data if they are not negligible. We have developed a new code to monitor and remove DC offsets. To obtain correct DC offset levels and noise levels, the offsets can be best removed using I/Q signals during the receive-only period, *i.e.*, during each clear frequency search stage. We have implemented the new code in the current radar operating system, installed it at the SENSU Syowa radars, and have been obtaining and removing DC offset values continuously since October 2001.

1. Introduction

The Super Dual Auroral Radar Network (SuperDARN) (Greenwald *et al.*, 1995), a network of high-frequency (HF) radars (Greenwald *et al.*, 1985), is a powerful tool used mainly for measuring plasma motions in the ionospheric E- and F-regions in vast fields-of-view that cover most of the polar regions of both hemispheres.

The radars adopt a multi-pulse sounding technique (Farley, 1972) that is specially designed to yield auto-correlation functions (ACFs) of received signals (receiver (Rx) output) using a radar operating system (software) ("ROS") and to obtain physical parameters, such as echo power, line-of-sight (LOS) Doppler velocity and Doppler spectral width, using a real-time "fitacf" algorithm in the ROS (Baker *et al.*, 1988). Cross-correlation functions (XCFs) between the signals received by the main array and those by an interferometer array can also be determined to measure the angles of arrival (elevation angles of received signals) when the interferometer array is available.

DC offsets in the quadrature outputs of the receiver (*i.e.*, I (in-phase) and Q (quadrature-phase) signals) must be properly detected and removed because the existence of non-zero I/Q DC offsets causes systematic errors in the estimation of ACFs, XCFs and the physical parameters in the fitacf algorithm (Yamagishi *et al.*, 1999) as well as in the estimation of echo power (I^2+Q^2) and phase (arctan(I/Q)) using a new raw time series analysis method (Yukimatu and Tsutsumi, 2002). However, the current hardware and software of the SuperDARN radar system does not contain a DC offset removal mechanism. Therefore, we have developed a code to monitor and remove I/Q DC offsets in the ROS (software). We describe the details of this code in the present report.

2. I/Q DC offsets and removal methods

2.1. *I/Q DC offsets*

We will denote the following variables:

- t: time,
- $I_1(t)$: I signal in the main receiver,
- $Q_1(t)$: Q signal in the main receiver,
- $I_2(t)$: I signal in the interferometer receiver,
- $Q_2(t)$: Q signal in the interferometer receiver,
- I_{j0}: DC offset in I_j signal ($j=1, 2$),
- Q_{j0}: DC offset in Q_j signal ($j=1, 2$),
- $Z_j(t)$: a complex signal constructed by I_j and Q_j ($j=1, 2$),
- $\langle A \rangle$: ensemble average of a variable, A,
- A^*: a complex conjugate of A,

and define the following relations:

$$I_{jc}(t) = I_j(t) - I_{j0}, \tag{1}$$
$$Q_{jc}(t) = Q_j(t) - Q_{j0}, \tag{2}$$
$$Z_j(t) = I_j(t) + iQ_j(t), \tag{3}$$
$$Z_{j0} = I_{j0} + iQ_{j0}, \tag{4}$$

where $i=\sqrt{-1}$, and $j=1$ or 2.
ACF and XCF can then be defined as

$$\mathrm{ACF}(\tau) = \langle Z_1(t) \cdot Z_1^*(t+\tau) \rangle, \tag{5}$$
$$\mathrm{XCF}(\tau) = \langle Z_1(t) \cdot Z_2^*(t+\tau) \rangle, \tag{6}$$

where τ is time lag.

In the fitacf algorithm, the "apparent" ACF and XCF (denoted as "$\mathrm{ACF_a}$" and "$\mathrm{XCF_a}$" in cases where the DC offsets are not taken into account and removed) are obtained as follows:

$$\mathrm{ACF_a}(\tau) = \langle Z_1(t) \cdot Z_1^*(t+\tau) \rangle, \tag{7}$$
$$\mathrm{XCF_a}(\tau) = \langle Z_1(t) \cdot Z_2^*(t+\tau) \rangle. \tag{8}$$

The relationships between the apparent and the true (correct) values for ACF and XCF (denoted as "$\mathrm{ACF_c}$" and "$\mathrm{XCF_c}$") can be described as follows:

$$\begin{aligned}\mathrm{ACF_a} &= \langle Z_{1a}(t) \cdot Z_{1a}^*(t+\tau) \rangle \\ &= \langle (Z_{1c}(t) + Z_{10}) \cdot (Z_{1c}^*(t+\tau) + Z_{10}^*) \rangle \\ &= \mathrm{ACF_c} + Z_{10}^* \cdot \langle Z_{1c}(t) \rangle + Z_{10} \cdot \langle Z_{1c}^*(t+\tau) \rangle + |Z_{10}|^2,\end{aligned} \tag{9}$$

$$\begin{aligned}\mathrm{XCF_a} &= \langle Z_{1a}(t) \cdot Z_{2a}^*(t+\tau) \rangle \\ &= \langle (Z_{1c}(t) + Z_{10}) \cdot (Z_{2c}^*(t+\tau) + Z_{20}^*) \rangle \\ &= \mathrm{XCF_c} + Z_{20}^* \cdot \langle Z_{1c}(t) \rangle + Z_{10} \cdot \langle Z_{2c}^*(t+\tau) \rangle + Z_{10} \cdot Z_{20}^*,\end{aligned} \tag{10}$$

where

$$Z_{ja}(t)=I_j(t)+iQ_j(t), \quad (j=1, 2) \tag{11}$$

$$Z_{jc}(t)=I_{jc}(t)+iQ_{jc}(t)=Z_{ja}(t)-Z_{j0}, \quad (j=1, 2) \tag{12}$$

$$ACF_c=\langle Z_{1c}(t)\cdot Z_{1c}^*(t+\tau)\rangle, \tag{13}$$

$$XCF_c=\langle Z_{1c}(t)\cdot Z_{2c}^*(t+\tau)\rangle. \tag{14}$$

On the other hand, in the raw time series analysis, a simple (and rough) estimation of the apparent echo power and phase ("PWR_a" and "PH_a") can be obtained using the equations

$$PWR_a=I_j^2+Q_j^2, \tag{15}$$

$$PH_a=\arctan(I_j/Q_j). \quad (j=1 \text{ or } 2) \tag{16}$$

However, the correct echo power ("PWR_c") and phase ("PH_c") should be calculated using the equations

$$PWR_c=(I_j-I_{j0})^2+(Q_j-Q_{j0})^2, \tag{17}$$

$$PH_c=\arctan((I_j-I_{j0})/(Q_j-Q_{j0}))+2n\pi. \quad (j=1 \text{ or } 2,\ n\text{: integer}) \tag{18}$$

In both methods, if $|Z_{j0}|$ (I_{j0} or Q_{j0}) ($j=1$ or 2) is not negligible compared with I_{jc}, Q_{jc}, $|ACF_c|$ or $|XCF_c|$, the DC offsets cause systematic errors in the estimation of physical parameters (noise level, echo power, LOS velocity, spectral width and elevation angle, *etc.*) and can also result in a lower echo detectability, especially for smaller echo powers. We should also note that the elevation angle measurement is especially sensitive to errors caused by the I/Q DC offsets and the frequency dependency of the phase differences between two receivers.

The "fitacf" algorithm can also be described from another point of view. Before the algorithm fits the ACFs to deduce the physical parameters, it determines the "noise ACF (ACF_N)" and subtracts the ACF_N from all the ACFs for all the range gates (Baker *et al.*, 1988). ACF_N is the average value of the ACFs at (a maximum of) 10 range gates where the lag-0 power (*i.e.*, $ACF(\tau=0)$) is the smallest among all the observed range gates in a single beam integration time. Therefore, ACF_N is expected to include the DC offset effect, and the process of subtracting the ACF_N seems to remove all the DC offset effects on the ACFs at all the range gates. However, this conclusion is not true because the process can remove the last term in eq. (9), *i.e.*, $|Z_{10}|^2$, but the second and third terms in eg. (9), *i.e.*, the effect of the cross terms, differ from range to range; thus, the process cannot remove the effect properly for all ranges. Consequently, the fitacf algorithm suffers from the I/Q DC offset effect unless the offsets are properly removed before constructing the ACFs and XCFs.

2.2. Removal methods

One proposal for removing the DC offsets is to subtract a real part of the ACF averaged over the time lag from each ACF (Greenwald, 2001). However, this method may also subtract real echoes with an LOS velocity close to zero. Such echoes could be produced by, for example, ground backscatters or low ionospheric plasma convective flows. Moreover, if the ensemble average is calculated over large samples, *i.e.*, if the ACFs are averaged over enough long periods, eq. (9) ideally yields

$$ACF_a \sim ACF_c + |Z_{10}|^2. \tag{19}$$

Thus, this method seems to work. In real observations, however, the ACFs are obtained using a limited number of samples. As a result, the cross-term effect (*i.e.*, the second and the third terms) in eq. (9) does not vanish, so eq. (19) is not always correct and the imaginary part of the ACFs (ACF_a in eq. (9)) can also suffer some DC offset effects as a result. Furthermore, the average value of ACF_c is not always guaranteed to be zero. Therefore, this method can not completely and properly remove all of the DC offset effects from the ACFs and is not suitable for studies using ground backscatters, such as research on gravity waves (*e.g.*, Samson *et al.*, 1989).

Determining the I/Q DC offsets using an averaged value of I/Q signals during each pulse sequence or during over the beam integration time period is another possible method for removing the I/Q DC offsets more properly:

$$I_{j0} = \langle I_j \rangle_{Tx},\ Q_{j0} = \langle Q_j \rangle_{Tx}, \qquad (j = 1, 2) \tag{20}$$

where $\langle\rangle_{Tx}$ is an average during a pulse sequence or a beam integration time.
The previous method did not separately determine the I/Q DC offset values. The present method, however, does attempt to precisely determine and remove the I/Q DC offset values from all the I/Q samples before constructing the ACFs and XCFs. Therefore, this method provides more accurate and reliable results.

However, the DC offsets can be difficult to distinguish from ground backscatters, especially in cases where the ground backscatter consists of an echo with a maximum power among all the range gates, as often happens. Moreover, from the "central limit theorem" in statistics, the standard deviation of the I and Q signals (I_j, Q_j $(j=1, 2)$) over the beam integration time ($\sigma_{\langle I_j \rangle}$, $\sigma_{\langle Q_j \rangle}$ $(j=1, 2)$) is as follows:

$$\begin{aligned} \sigma_{\langle I_j \rangle} &= \sigma_{I_j} / \sqrt{n} \\ &\cong \sigma_{I_j} / \sqrt{2 \times 10^4} \\ &\cong \sigma_{I_j} / 140, \qquad (j = 1, 2) \end{aligned} \tag{21}$$

where

σ_{I_j}: standard deviation of I_j signals during a beam integration time
($|I_j| \leqq 2^{11}$, $0 \leqq \sigma_{I_j} \leqq 2^{11} \cong 2 \times 10^3$ (in case of signed 12-bit A/D))
$\sigma_{\langle I_j \rangle}$: standard deviation of $\langle I_j \rangle_{Tx}$
(averaged values of I_j during each beam integration time)
n: number of averaging (typically $300 \times 70 \cong 2 \times 10^4$)
(n is dependent on the sounding modes
(*e.g.*, pulse pattern, integration time.)).

The values of $\sigma_{\langle I_j \rangle}$ and $\sigma_{\langle Q_j \rangle}$ can be large, depending on the amount and the intensity of the real ionospheric and ground backscatters, and will also vary with time (over both short and long time scales). In other words, the precision of the DC offsets may be unstable. Therefore, this method is not the most reliable solution for our purposes.

2.3. New removal method

Determining the I/Q DC offsets using an averaged value of I/Q signals during a non-transmission (receive-only, non-Tx or Rx-only) period is a much better solution for

determining the correct DC offsets than the previously described methods because the signals are not affected by any ionospheric or ground backscatters from transmitted pulses, whose values can have large, undesirable standard deviations, although some unexpected and temporal interference noises may still be present. In real operation mode in ROS, there is a non-Tx period called the "clear frequency search (fclr)" stage. During this period, without any pulse transmissions, a limited number of I and Q signals are sampled for a specified 300-kHz frequency band, typically in 5-kHz steps, to determine the quietest frequency and ensure a minimal received noise level. If we could determine the average (expected) values of the I and Q signals at the quietest (chosen) frequency during the fclr stage, these values would represent the expected I and Q DC offsets. This relationship can be expressed as follows:

$$I_{j0}=\langle I_j\rangle_{fc},\ Q_{j0}=\langle Q_j\rangle_{fc}, \qquad (j=1, 2) \tag{22}$$

where $\langle\rangle_{fc}$ is average during the non-Tx (Rx-only) "fclr" stage.
The relationship between the I/Q signals and the noise level is as follows:

$$\sigma_{I_j}=\sqrt{\langle(I_j-I_{j0})^2\rangle_{fc}}=\sqrt{\langle I_j^2\rangle_{fc}-I_{j0}^2}, \qquad (j=1, 2) \tag{23}$$

$$\sigma_{Q_j}=\sqrt{\langle(Q_j-Q_{j0})^2\rangle_{fc}}=\sqrt{\langle Q_j^2\rangle_{fc}-Q_{j0}^2}, \qquad (j=1, 2) \tag{24}$$

$$N_c=\sigma_{I_i}{}^2+\sigma_{Q_i}{}^2=N_{app}-(I_{i0}{}^2+Q_{i0}{}^2)=N_{app}-|Z_{i0}|^2, \tag{25}$$

and

$$\sigma_{I_j}=\sigma_{Q_j}, \qquad (j=1, 2) \tag{26}$$

(this is valid statistically, *i.e.*, if the number of averaged items is sufficiently large and the gains of the I and Q channels are exactly the same)
i.e.,

$$\sigma_{I_i}=\sigma_{Q_i}=\sqrt{N_c/2} \tag{27}$$

where

σ_{I_j}: standard deviation of I_j signals during the fclr stage ($j=1, 2$),
σ_{Q_j}: standard deviation of Q_j signals during the fclr stage ($j=1, 2$),
N_c: true (correct) Noise value,
N_{app}: apparent noise level ($=\langle I_i{}^2+Q_i{}^2\rangle_{fc}=\langle I_i{}^2\rangle_{fc}+\langle Q_i{}^2\rangle_{fc}$).

However, the number of samples during a typical fclr stage is typically only 200. So, I_{j0} and Q_{j0} in eq. (22) scatter statistically (even if the DC offset level is temporally constant), *i.e.*, they must be treated as "random variables". According to the central limit theorem, they will produce a normal (Gaussian) distribution such that

$$\sigma_{\langle I_j\rangle}=\sigma_{I_j}/\sqrt{num}=\sigma_{I_j}/\sqrt{200} \tag{28}$$

$$\sigma_{\langle Q_j\rangle}=\sigma_{Q_j}/\sqrt{num}=\sigma_{Q_j}/\sqrt{200} \tag{29}$$

where

$\sigma_{\langle I_j\rangle}$: standard deviation of $\langle I_j\rangle_{fc}$,
$\sigma_{\langle Q_j\rangle}$: standard deviation of $\langle Q_j\rangle_{fc}$,
num: number of averaged items,

and from eq. (26),

$$\sigma_{\langle I_1\rangle}=\sigma_{\langle Q_1\rangle}=\sqrt{N_c/2}/\sqrt{200}=\sqrt{N_c}/20. \tag{30}$$

If $N_c \cong 2000$ (a typical value for many SuperDARN radars using a 12-bit A/D card),

$$\sigma_{\langle I_1\rangle}=\sigma_{\langle Q_1\rangle}=\sqrt{N_c}/20 \cong 2.2. \tag{31}$$

This means that if we determine the I/Q DC offsets from the average I/Q values during the fclr stages, the values can vary with time with a standard deviation of $\sim 2\times\sqrt{N_c/2000}$. This value is not always negligible and is rather dependent on noise levels. The above statistical variation also introduces a new undesired "noise" into the real I/Q signals, even when the real DC offsets are well tuned and exactly equal to zero.

Considering the above, we can conclude that a realistic solution for determining the I/Q DC offsets is to calculate the statistical expectation (average) values of a sufficiently large number of 200-sample I/Q averages during each fclr stage; that is to say,

$$I_{j0}=\langle\langle I_j\rangle_{fc}\rangle,\ Q_{j0}=\langle\langle Q_j\rangle_{fc}\rangle, \qquad (j=1, 2) \tag{32}$$

(ensemble averages of $\langle I_j\rangle_{fc}$, $\langle Q_j\rangle_{fc}$ over a sufficiently large number of fclr stages.) Fortunately, the I/Q DC offset values are normally expected to vary slowly with time because of, for example, the slow diurnal temperature variation in the radar observation hut where the receivers are located. Therefore, we can replace the ensemble average by a temporal average for a sufficiently long period and can adopt the temporal average of the 200-sample I/Q averages as the true (or expected) I/Q DC offset.

3. Development of new DC offset monitoring and removal code

To realise the new I/Q DC offset monitoring and removal method described in the previous section, the following points should also be considered to create a better algorithm for real-time programming in ROS.

1) the number of 200-average I,Q data points kept in the computer memory should be reduced for faster calculation and lower CPU load (though average values must be calculated using a sufficiently large number (*e.g.*, 100) of data points),
2) the older 200-sample average values should be rather less contributive,
3) apparent large temporal jumps in DC offset values ($\langle I\rangle$ and $\langle Q\rangle$), due to unexpected, abrupt large interference noise during the fclr stage, should be avoided, and
4) the CPU load should be reduced as much as possible.

In view of the above, we introduced "oblivion coefficients (*obliv*)" to improve the algorithm for determining the real DC offset values so that only the latest (most recent) DC offset value and the latest standard deviation of the averaged I,Q signals for each I,Q channel for every frequency band need to be kept in the computer memory (RAM). (This method can be validly applied here because the DC offsets are expected to change very slowly and smoothly with time). The DC offset values are obtained as follows:

$$I_{j0now}=obl\nu \cdot I_{j0last}+(1\text{-}obl\nu)\cdot\langle I_j\rangle_{now}, \qquad (j=1, 2) \tag{33}$$

where

$$0<obl\nu<1. \tag{34}$$

Note that

$$oblv = oblv_1 = e.g.,\ 0.90, \quad \text{if } |\langle I_j\rangle_{now} - I_{j0last}| \leqq 3\sigma_{\langle I_j\rangle last}; \quad \text{otherwise, } oblv = oblv_2 = e.g.,\ 0.99\ (> oblv_1), \text{ and} \tag{35}$$

$$oblv_1 < oblv_2, \tag{36}$$

$$\sigma_{\langle I_j\rangle now} = \sqrt{\langle(\langle I_j\rangle_{fc} - \langle\langle I_j\rangle_{fc}\rangle)^2\rangle_{now}} = \sqrt{\langle\langle I_j\rangle_{fc}^2\rangle_{now} - \langle\langle I_j\rangle_{fc}\rangle_{now}^2} = \sqrt{\langle\langle I_j\rangle_{fc}^2\rangle_{now} - I_{j0now}^2}, \tag{37}$$

$$\langle\langle I_j\rangle_{fc}^2\rangle_{now} = oblv_{now} \cdot \langle\langle I_j\rangle_{fc}^2\rangle_{last} + (1 - oblv_{now}) \cdot \langle I_j\rangle_{fc}^2{}_{now}, \tag{38}$$

where

I_{j0now}: present real (expected) DC offset value to be determined,
$\langle I_j\rangle_{now}$: present 200-sample-average of I/Q signals during a fclr stage,
I_{j0last}: DC offset value determined in the last fclr stage,
$\sigma_{\langle I_j\rangle last}$: standard deviation of the $\langle I_j\rangle_{fc}$ (not I_j) at the last time,
$\sigma_{\langle I_j\rangle now}$: current standard deviation of the $\langle I_j\rangle_{fc}$ (not I_j),
$\langle\langle I_j\rangle_{fc}^2\rangle_{now}$: current average of $\langle I_j\rangle_{fc}^2$.

As the DC offsets may depend on the operating frequency, we divided the 8-20 MHz SuperDARN operating frequency band into 24 sub-bands in 0.5-MHz steps and used only the offset values in the same frequency sub-band to calculate the expected DC offsets. Using this algorithm and, for simplicity, the case where *oblv* is constant (*i.e.*, equal to $oblv_1$ (*e.g.*, 0.9)),

$$\text{DCoffset(m)} = (1\text{-}oblv) \sum_{k=0}^{\infty} (oblv)^k \cdot \text{DCoffset(m-k)}, \tag{39}$$

which means that the contribution of the older DCoffsets vanishes exponentially (if the DCoffset value is assumed to be almost constant or vary only very slowly with time, without any unexpected temporal jumps). In other words, the past DC offset values are averaged with a weighting function, like in eq. (39), so that the older values are less influential or "forgotten" (more "oblivious") in an exponential manner. The first oblivion coefficient, $oblv_1$, was selected so that the temporal variation of I_{j0now} in eq. (33), *i.e.*, the expected DC offset value, would be within 1 A/D unit and could quickly follow the expected real DC offset variations (*e.g.*, temporal variations in room temperature, *etc.*) over a time scale of typically several minutes. The relationship in eq. (36) (*i.e.*, $oblv_2 > oblv_1$) is for reducing the effect of unexpected large interference noises. However, the second oblivion coefficient, $oblv_2$, should not exactly equal 1.0 because of the possibility of sudden (manual or unexpected) changes in the real DC offset values for safety. The value, $oblv_2$, determines the time constant for the calculated DC offset values following such sudden changes (although the time constant with this method also depends on the beam integration time and the operating frequency sequences, such as the fixed frequency mode, frequency scan mode, or frequency optimization mode that allows arbitrary jumps in frequency sub-bands).

The current "fclr" function in the ROS only samples 2 A/D channels (the I and Q outputs for the main receiver) to determine the noise level for each test frequency. However, our new "fclr" function uses all 4 A/D channels (the I/Q channels for the main receiver and the ones for the interferometer receiver) to determine all 4 DC offsets.

Furthermore, the real-time DC offset values for the 4 A/D input channels (both the instantaneous 200-sample average and the statistical expected value) can be seen on the "tdisplay (real-time ROS quick-look program)" screen (updated for every beam integration time) and the (measured and expected) DC offset values (*i.e.*, $\langle I \rangle_{fc}$ and $\langle\langle I \rangle_{fc}\rangle$) are recorded in very small ".ofs" files for later analysis (if desired). After the obtained DC offset values are subtracted from the I and Q signals, the corrected noise values are determined using our new fclr function. The corrected I and Q sample data are then passed to the functions that construct the ACFs and XCFs, as in the present ROS; the constructed ACFs and XCFs are then passed to the fitacf algorithm. The corrected I and Q samples are also passed to functions that form and process the raw time series.

We developed a code to monitor, remove and record the DC offsets in real-time for the previous radar operating system (called RADOPS/2000) and have migrated this code to the present system (RST/ROS). The new code was installed in August 2001 at the Syowa South and East HF Radars of NIPR for the SuperDARN (SENSU) systems located at Syowa station, Antarctica. The code has been obtaining and removing DC offset values continuously since October 2001.

4. Initial results

Here, we present some initial results obtained with the new DC offset monitoring and removal code installed in the SENSU Syowa radar systems.

Figure 1 shows an example of the one-day DC offset variation in the I channel of the main receiver obtained at SENSU Syowa South radar on Aug. 20, 2001. Each horizontal axis represents the universal time (UT) in hours, and each vertical axis represents the channel output in 12-bit A/D units (12-bit (4096) corresponds to ± 10 V).

Figure 1A shows the one-day variation of the simple 200-sample-average values during each fclr stage, which corresponds to I_{10} in eq. (22). Figure 1B shows the standard deviation of I_0, which shows that the 200-sample-averages scatter over several A/D units. Figure 1C is the DC offset of the channel determined using the method described in the previous section. The temporal variation in DC offset values is stable with time (within $\sim$1 A/D unit) over a short time period and properly determined.

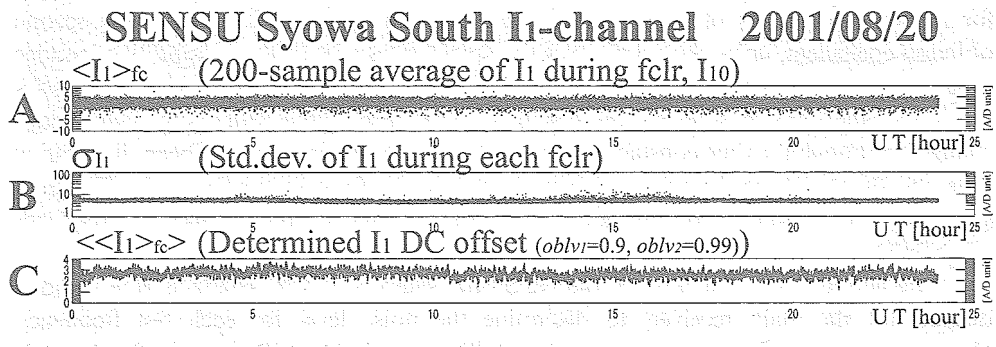

Fig. 1. An example of the one-day DC offset data for the I channel of the main receiver, obtained by the SENSU Syowa South radar on August 20, 2001. The horizontal axes represent the universal time in hours. See the text for details.

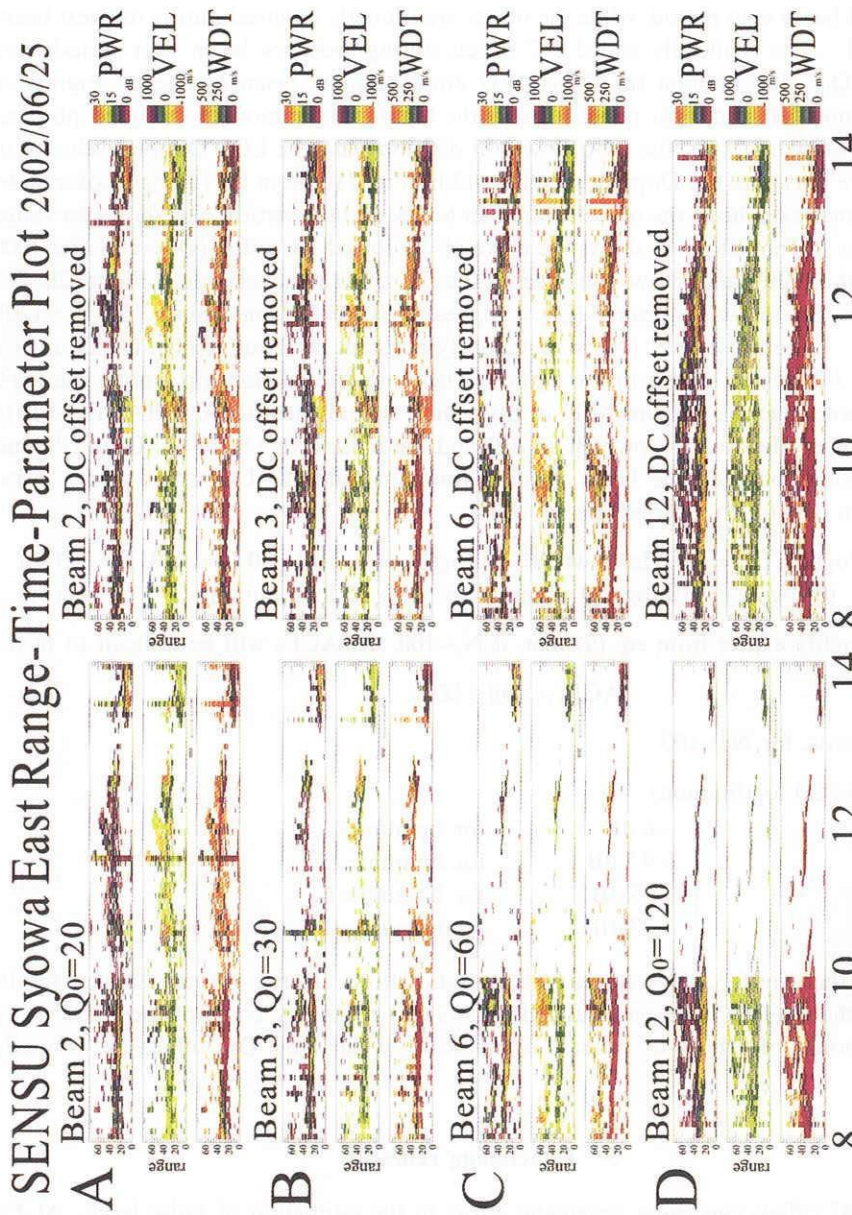

Fig. 2. Effect of the DC offset removal method on data obtained at the SENSU Syowa East radar between 0800 and 1400 UT on June 25, 2002. See the text for details.

Figure 2 shows the effect of the DC offset removal method on results obtained at the SENSU Syowa East radar between 0800 and 1400 UT on Jun. 25, 2002. The DC offsets are always removed up until 1000 UT. After 1000 UT, two beam scan periods are repeated so that the DC offsets are forced to be added to each I and Q channel during the first normal beam scan period, while the offsets are properly removed during the next beam scan period. The artificially added DC offsets during each first beam scan period were $I_{10}=0$ and $Q_{10}=10\times$bmnum (in 12-bit A/D units, bmnum: beam number). Figure 2A (the uppermost left and right panels) shows the temporal variation of the fitted physical parameters of beam 2, *i.e.*, the echo power in dB (top bar), the LOS Doppler velocity in m/s (middle bar), and the Doppler spectral width in m/s (bottom bar) using a color code. The horizontal axis shows the universal time in hours, and the vertical axis shows the range gate number. The left panel shows the effect of the forced DC offset ($Q_{10}=20$) after 1000 UT, while the right panel shows the effect of the DC offset removal code. Figure 2B, 2C, and 2D show the results for beam 3 ($Q_{10}=30$), beam 6 ($Q_{10}=60$), and beam=12 ($Q_{10}=120$), respectively. The noise level (N_c) was relatively constant at about 100 (in (A/D unit)^2), throughout the period shown in the figure. Therefore, the relationship among the lag-0 power (denoted here as "lag0pwrdB" in dB, which is equivalent to 10 log(ACF($\tau=0$))), the echo power (denoted as "pwrdB" in dB) and the noise level (N_c in (A/D unit)^2), and the relationship between the beam number (bmnum) and the DC offset power ($10\times$ log($|Z_{10}|^2$) in dB) for this period are as follows:

$$10\ \log(\mathrm{ACF}(\tau=0))=\mathrm{lag0pwrdB}=10\ \log(N_c)+\mathrm{pwrdB}=20+\mathrm{pwrdB}, \tag{40}$$

$$10\ \log|Z_{10}|^2=10\ \log((10\times\mathrm{bmnum})^2)=20+20\ \log(\mathrm{bmnum}). \tag{41}$$

We can roughly expect from eq. (9) that, if $N_c\sim100$, the ACFs will be difficult to fit if

$$|\mathrm{ACF}(\tau=0)|\lesssim|Z_{10}|^2. \tag{42}$$

In other words, for Nc$\sim$100,

$$\mathrm{pwrdB}\lesssim 20\ \log(\mathrm{bmnum})$$

$$=\begin{cases}\sim 6\ \mathrm{dB} & \text{for bmnum}=2\\ \sim 9.5\ \mathrm{dB} & \text{for bmnum}=3\\ \sim 15\ \mathrm{dB} & \text{for bmnum}=6\\ \sim 22\ \mathrm{dB} & \text{for bmnum}=12.\end{cases} \tag{43}$$

We can see that Fig. 2 roughly agrees with our estimation. Hence, we can use these results to confirm that the DC offset removal code works very effectively, enabling the detectability and the amount of echoes to increase dramatically when large DC offsets are properly removed.

5. Concluding remarks

I/Q DC offsets can cause systematic errors in the estimation of noise levels, ACFs, XCFs, and fitted physical parameters, such as the echo power, LOS Doppler velocity, Doppler spectral width and elevation angle, and also in the estimation of echo power and phase in raw time series analyses. Therefore, we have developed a new code to monitor,

determine remove and record the I/Q DC offset values for the SuperDARN ROS. This code determines the DC offsets during the Rx-only fclr stage prior to constructing the ACFs and XCFs or before the raw time series analysis and seems to work well. This method will increase the accuracy of SuperDARN fitted physical parameters (especially elevation angles) as well as the ACFs, XCFs and echo power and phase in raw time series. Consequently, the code will increase the detectability and the amount of observed echoes, especially those with a smaller power that is close to the maximum among noise level and DC offset power ($|Z_0|^2$).

However, this method has one limitation in that the calculated DC offsets follow the real DC offset values by a certain time constant if a large, unexpected or manual change in the DC offsets occurs. Furthermore, our method only uses 200-sample data points at the selected operating frequency in each fclr stage. If a smaller time constant of the DC offset values is desired, we should average a larger number of I/Q samples during each fclr stage in order to make the average values be statistically more stable. In the typical fclr stage, the five quietest frequencies out of all 60 5-kHz-step frequencies in the 300-kHz frequency band are selected during the first fclr stage in order to pass them to the second fclr stage for choosing the real quietest frequency. Therefore, the 200 samples obtained for each of these five frequencies during the second fclr stage could then be used to obtain 1000 samples (200 samples/frequency$\times$5 frequencies$=$1000 samples) in order to determine the 1000-sample I/Q average that is statistically more stable than the 200-sample I/Q average. Alternatively, the 50 samples in each of the 60 frequencies in the first fclr stage could also be added to the 200 samples in each of the 5 quietest frequencies (as determined in the first fclr stage) measured in the second fclr stage to obtain 4000 samples (50 samples/frequency$\times$60 frequencies (in the first fclr stage)$+$200 samples/frequency$\times$5 frequencies (in the second fclr stage)$=$4000 samples). These methods assume that the DC offsets are almost completely constant within the narrow 300-kHz frequency band. Our method makes this assumption and divides 8–20 MHz band into 24 sub-bands in 500-kHz steps; the above methods also seem to work and might be a better solution. However, the above methods will be affected by possible interference noises more frequently, especially in noisy environments. Our method can be more safely used even in noisy environments, with the above limitation. Nevertheless, using all 1000 samples obtained at the five quietest frequencies might also be a good solution.

Some SuperDARN radar studies have reported that the DC offsets depend on the attenuation levels (as well as the operating frequencies). We feel that this should not occur unless some of the local oscillator signals leak into the IF stage in the receiver, or a similar error occurs. However, since our method can be easily used to determine the DC offset levels for every attenuation level, we will add such a function to our new code in the near future. Recently, some discussion regarding the replacement of the 12-bit A/D card with a 16-bit A/D card has arisen in the SuperDARN community. If this replacement occurs and the input level (gain) of the A/D card does not change, the DC offset values will increase by 16 times. To take advantage of the higher resolution A/D card and to improve the detectability of weaker echoes, the precision (the effective number of averaging) of our DC offset removal code will need to be increased so that the statistical deviation is small enough ($<$1 A/D bit). Theoretically, this should not present a problem and can

be accomplished with a minor modification of the code.

Acknowledgments

The authors are grateful to K.B. Baker of the National Science Foundation, M. Pinnock of the British Antarctic Survey, and W.A. Bristow and J. Hughes of the University of Alaska, Fairbanks, for their helpful discussions. This research was supported by a Grant-in Aid for Scientific Research (A: 11304029) from the Japan Society for the Promotion of Science (JSPS). The Ministry of Education, Culture, Sports, Science and Technology supports the SENSU Syowa HF radar systems. The 36th-42nd Japanese Antarctic Research Expeditions (JAREs) have performed all of the HF radar operations at Syowa. We especially thank all the JARE members who contributed to the construction and operation of the HF radar systems at Syowa Station.

The editor thanks Dr. T. Ogawa for his help in evaluating this paper.

References

Baker, K.B, Greenwald, R.A., Villain, J.P and Wing, S. (1988): Spectral characteristics of high frequency (HF) backscatter from high latitude ionospheric irregularities: Preliminary analysis of statistical properties. RRADC-TR-87-284, Rome Air Development Center, Griffis Air Force Base, NY.

Farley, D.T. (1972): Multi-pulse incoherent scatter correlation function measurements. Radio Sci., **7**, 661-666.

Greenwald, R.A., Baker, K.B., Hutchins, R.A. and Hanuise, C. (1985): An HF phased-array radar for studying small-scale structure in the high latitude ionosphere. Radio Sci., **20**, 63-79.

Greenwald, R.A., Baker, K.B., Dudeney, J.R., Pinnock, M., Jones, T.B., Thomas, E.C., Villain, J.-P., Cerisier, J.-C., Senior, C., Hanuise, C., Hunsucker, R.D., Sofko, G., Koehler, J., Nielsen, E., Pellinen, R., Walker, A.D.M., Sato, N. and Yamagishi, H. (1995) DARN/SuperDARN: A global view of the dynamics of high-latitude convection. Space Sci. Rev., **71**, 761-796.

Greenwald, R.A. (2001): Impact of combined ground-scatter and ionospheric returns on SuperDARN velocity estimation. presented at SuperDARN 2001 workshop in Venice.

Samson, J.C., Greenwald, R.A., Ruohoniemi, J.M. and Baker, K.B. (1989): High-frequency radar observations of atmospheric gravity waves in the high-latitude ionosphere. Geophys. Res. Lett., **16**, 875-878.

Yamagishi, H., Yukimatu, A.S. and Maegawa, K. (1999): How does the DC offset of the receiver output affect the echo detection by RADOPS? -A test with an echo simulator-. presented at SuperDARN 1999 workshop in Reykjavik.

Yukimatu, A.S. and Tsutsumi, M. (2002): A new SuperDARN raw time series analysis method and its application to mesopause region dynamics. Geophys. Res. Lett., **29** (20), 1981, doi: 10.1029/2002GL015210.

(Received June 5, 2002; Revised manuscript accepted July 2, 2002)